Chapter 4

Observations and data analysis

A large number of CDS observations were planned and executed. Most of them were made during three periods (totalling more than two months) in which the author was, together with B. Bromage, at the SOHO operation centre at Goddard Space Flight Center (GSFC), Greenbelt, MD, USA. Most of the observations were acquired during August-September 1996 and September-October 1997. In many cases, the CDS observations have been supported by observations with the other SOHO instruments, and by ground based observatories. All the raw data are now in publicly available databases on the WWW.

The first Section (4.1) of this Chapter describes some of the CDS studies that were developed to study coronal holes with CDS, to give an idea of the type of problems CDS observations of coronal holes have posed. The following Sections briefly describe some of the observations that have been taken during the period 1996-1998, excluding the calibration studies, already described in Chapter 3. The CDS instrument has successfully produced a wealth of data of all different types, incomparable to anything obtained in the past. For example, the data collected for this thesis, listed in Table B.1, amounts to several G-bytes. This has posed new problems in, for example, the storage and analysis of such large datasets. Note that most of the data obtained have been partly analysed or at least examined. The results presented in this thesis are from a selected subset of these data.

Section(4.5) presents the methods and the software that were developed by the author to tackle some of the problems encountered in the data analysis.

4.1 Some of the CDS studies used or developed

Most of the CDS studies already available (and used by most people) used the smallest slits ($2''$x$2''$ or $2''$x$240''$). A preliminary analysis of many observations was performed, and showed that the small slits, contrary to expectation, were *not* producing any significant increase in spectral resolution compared to the larger 4″ slits. The only advantage is the spatial resolution, but at the expense of losing half the signal. This fact, together with short exposure times, made almost all the CDS studies already present in the CDS database unsuitable for coronal hole observations, simply because of the low signal.

Many CDS studies were therefore designed and developed by the author and B. Bromage. The design of a study has to take into account and balance exposure times, telemetry, number and width of the extraction windows, use of different slits, movements of the mirror and solar rotation, just to mention a few, and is quite complex. It is not possible to describe in detail the pros and cons of each type of study. However, Table 4.1 lists a few of the CDS studies used by the author, just to give an idea of the various possibilities offered by CDS. Table 4.2 lists the principal lines observed by some of the most commonly used studies, which can be grouped into these types:

- **Large field of view**

  The largest area of the Sun that can be observed with a single NIS observation, is (4′x4′). One example is the CDS study LIMB which, with only a limited number of extraction windows, including lines emitted from the chromosphere to the corona, provides temperature and density information. The exposure time is kept low in order to have the total area observed say within an hour, to approximate a snapshot of the Sun. LIMB uses a 4″x240″ slit and a 30s exposure to build with 60 movements of the scan mirror a 4′x4′ raster. Only 15 lines are extracted, including chromospheric transition region and coronal lines, and the density diagnostic Si IX lines. The total duration of this study is 37 minutes. The restrictions of this study are a) the narrow spectral windows (20 pixels), which in some cases make it difficult to estimate the background, and b) the short exposure time.

  Another similar study is UCLAN_N4, more suitable for coronal hole observation than LIMB, because of the longer exposure time, larger windows and more diagnostic lines (at the expense of a longer duration).

  During the planning, a series of such observations were pointed so that the regions overlapped. This enabled a 'mosaic' of data to be formed, as explained in Section 4.5, giving an overall view over large portions of the Sun, with some density and temperature diagnostic lines included. The CDS daily synoptic study, SYNOP, is also made up of a series of 4′x4′ rasters, this time covering a N-S strip of the Sun centred on the meridian.

- **Medium field of view**

Table 4.1: *Some of the CDS studies developed or used (those already present in the database are marked with a *). Each line represents one or more 'study variation', depending on the exposure time, and telemetry rate, for example. (NR) indicates normal rate, while (HR) high-rate. Note that the indicated area covered by each NIS raster is not equivalent to the usable one, due to the slant of the spectra. All NIS studies also extracted 4 background windows. For the studies with data extraction windows, their number and the width in pixels of each window is given.*

study name	Sp	slit	exposure time (s)	area covered	duration	type of extraction	compression	comments
UCLAN_N2	NIS	4″x240″	160 (NR) - 80(HR)	120″x150″	2h30m (NR) - 1h09m (HR)	all lines	none	
UCLAN_N2	NIS	4″x240″	120 (NR) - 60(HR)	120″x150″	1h19m (NR) - 45m (HR)	all lines	sum (2 lines)	
UCLAN_N3	NIS	4″x240″	120 (NR) - 60(HR)	120″x180″	1h13m (NR) - 39m (HR)	12 windows (90 pix)	none	
UCLAN_N3	NIS	4″x240″	90 (NR) - 45(HR)	120″x180″	54m (NR) - 33m (HR)	12 windows (90 pix)	sum (2 lines)	
CHBOPT2	NIS	4″x240″	50 (NR)	60″x240″	1h (NR)	16 windows (35 pix)	none	complex raster
UCLAN_N4	NIS	4″x240″	60 (NR) - 30(HR)	240″x240″	1h10m (NR) - 39m (HR)	8 windows (45 pix)	none	
LIMB	NIS	4″x240″	30 (NR)	240″x240″	37m (NR)	8 windows (20 pix)	none	*
WIDE3LA1	NIS	90″x240″	25 (NR)	234″x240″	1m53s (NR)	He I, O V, Mg IX	none	* for movies
MOVIE	NIS	90″x240″	50 (NR)	90″x240″	1h (NR)	He I, O V, Mg IX	none	* 60 xeach position
NISAT	NIS	2″x240″	50 (NR)	20″x240″	1h (NR)	all lines	none	*
NISAT_S5	NIS	4″x240″	150 (NR) - 150(HR)	40″x240″	1h06m (NR) - 48m (HR)	all lines	none	
ARC_CALN	NIS	4″x240″	45 (NR)	32″x70″	13m (NR)	all lines	none	
DEM_GIS	GIS	4″x4″	20 (NR)	24″x24″	13m (NR)	all lines	none	*
NSGSCAN1	GIS	4″x4″	400 (NR)	4″x60″	1h40m(NR)	all lines	none	
EWGSCAN2	GIS	4″x4″	400 (NR)	120″x4″	3h20m (NR)	all lines	none	
G2AL/v2	GIS	4″x4″	400 (NR)	80″x4″	2h14m (NR)	all lines	none	
NSGSCAN2	GIS	4″x4″	400 (NR)	4″x120″	3h20m (NR)	all lines	none	
HRBNDWE	GIS	4″x4″	5 (HR)	60″x4″	2h48m (HR)	all lines	none	100 xeach position
MICRO_2	GIS	4″x4″	50 (HR)	20″x20″	22m (HR)	all lines	none	

Table 4.2: *Principal Selected Lines in the CDS/NIS Wavelength Bands. The lines observed by the different CDS studies are marked with a star. Wavelengths are taken from the CHIANTI database. When only one decimal place is indicated, the lines are blends of at least two transitions. The temperature of maximum ionization fraction is also indicated.*

Ion	Wavelength [Å]	log T_e [K]	NIS	LIMB	CHBOPT2
Fe XI	341.113	6.1	1		*
Si IX	341.9	6.0	1	*	*
Si IX	345.1	6.0	1		*
Fe X	345.722	6.0	1		*
Fe XII	346.852	6.1	1		
Si X	347.402	6.1	1		
Fe XIII	348.183	6.2	1		
Mg VI (bl Fe XI)	349.2	5.7	1	*	*
Si IX	349.9	6.0	1	*	*
Fe XII	352.106	6.1	1		*
Fe XI	352.662	6.1	1		*
Mg V	353.091	5.5	1		*
Si X	356.0	6.1	1		
Fe XI	356.519	6.1	1		
Ne IV (bl Fe XI)	358.7	5.3	1		
Ne V	359.4	5.5	1		
Fe XVI	360.761	6.4	1		
Mg VII	363.772	5.8	1		*
Fe XII	364.467	6.1	1		*
Mg VII	367.7	5.8	1	*	*
Mg IX	368.070	6.0	1	*	*
Fe XI	369.153	6.1	1		*
O III (bl N III)	374.0	5.1	1		
N III (bl O III)	374.4	5.1	1		
Si XII	520.665	6.3	2	*	*
O III	525.796	5.1	2		
C III (bl O II)	538.3	5.0	2		
Ne IV	541.128	5.3	2		*
Ne IV	542.072	5.3	2		*
Ne IV	543.891	5.3	2		*
Al XI	550.031	6.2	2		
O IV	553.329	5.3	2		
O IV	554.513	5.3	2		
O IV	555.263	5.3	2		
Ca X	557.765	5.8	2		*
Ne VI (bl Ne VII)	558.594	5.6	2		*
Ne VII	561.728	5.7	2		*
Ne VI	562.803	5.6	2		*
Ne V	569.8	5.5	2		
Ne V	572.3	5.5	2		
Ca X (bl O III)	574.0	5.8	2		
Ar VII	585.754	5.5	2		
O III	599.597	5.1	2		*
Si XI (II order)	303.324	6.2	2	*	*
He II (II order)	303.78	4.9	2	*	*
O IV	608.397	5.3	2	*	*
Mg X	624.941	6.0	2	*	*
O IV	625.853	5.3	2	*	*
O V	629.732	5.4	2	*	*

A smaller area is rastered, but more lines are obtained. The purpose of these observations was to study coronal holes in more detail, with a higher signal-to-noise and with lines suitable for DEM and element abundance analysis.

An example is the CHBOPT2 study, which is composed of a series of 3 adjacent rasters (slit $4''$x$240''$) of $20''$x$240''$ covering a total area of $1'$x$4'$. The CHBOPT2 was optimized to account for the lower sensitivity of the NIS 1 detector, compared with the NIS 2 one. For each $20''$x$240''$ raster, a series of NIS 2 windows with a 50s exposure time is extracted. Then, three $20''$x$240''$ rasters are repeated on the same region extracting only NIS 1 windows, with the aim of increasing the S/N to a level similar to that of NIS2 by averaging the exposures. Each $20''$x$240''$ raster lasts about 5 minutes, and the total duration of the study is about an hour. The drawback of this study is the lack of co-temporality between the observed intensity of NIS 1 and NIS 2 lines. A temporal variability of lower transition region line intensities over 5 minute time scales cannot be ruled out, as brightenings in the network. However, spatial averages over large areas would smooth out such variations.

Another study that was developed is UCLAN_N3, where a large portion of the NIS spectrum is extracted, to make use of all the diagnostic capabilities of CDS. With a relatively large area ($2'$x$3'$) covered, it typically observes the whole of a network cell.

- **Full rasters**

  In this case, the full NIS spectral range is recorded, at the expense of an even smaller area. The full raster studies provide enough spectral information to perform a more complete DEM analysis.

  Examples are the spectral atlas NISAT_S5 study, covering a small $40''$x$240''$ area, and UCLAN_N2. NISAT_S5 was designed by the author to raster a small ($40''$x$240''$) area with the $4''$x$240''$ slit and a long (150 s) exposure time. One drawback is that most of the time is spent telemetering the data (longer exposures are not possible because of the cosmic ray problem).

  A much better study is UCLAN_N2, a raster of $120''$x$150''$, that after the correction for the slant becomes $2'$x$2'$. In this case, the telemetry time is close to the exposure time and no time is 'wasted'.

4.2 The observations during August-September 1996

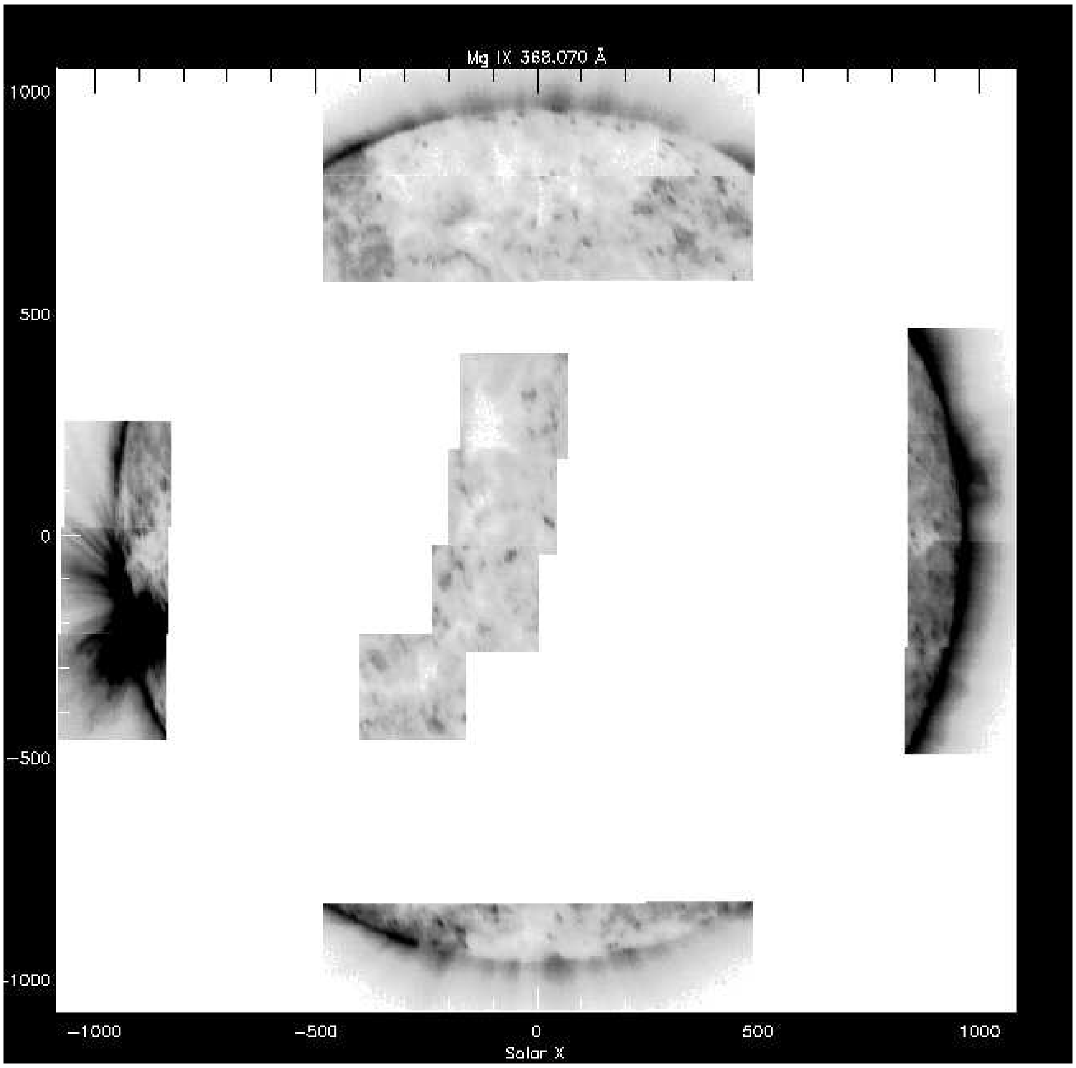

Figure 4.1: *A mosaic of Mg IX 368 Å monochromatic images (negative image) created from a series of CDS observations, centred around August 25th 1996. Note the extended North polar hole, the active region on the limb, and the Elephant's Trunk coronal hole in the centre.*

During 1996 the Sun was still around minimum activity, had extended polar coronal holes (see e.g. Figure 4.1), few active regions, and symmetric equatorial streamers. A SOHO campaign, called Whole Sun Month (WSM), was organised by S. Gibson and D. Biesecker to study the solar minimum corona between 1 and 3 $R_\odot$ for a whole solar rotation using all the SOHO instruments. One of the main goals was to then gather all this information in order to determine the large-scale physical properties (such as densities, temperatures) of the relatively simple azimuthally symmetric streamers, and the extended coronal holes.

August 1996 was chosen as the observation month, after a last minute change of plans. Since the first series of CDS observations for this thesis was planned in the same month, and since most of the scientific objectives were in common with the WSM campaign, some effort was spent by B. Bromage and the author (at GSFC for the whole month of August) in coordinating the two sets of observations. The CDS studies for the WSM campaign were developed by A. Fludra. Section 4.2.1 describes the observations that were carried out, which mainly concentrated on the two polar regions and the two east and west limbs. Figure 4.1 shows a mosaic including such observations.

The northern polar coronal hole was large and tilted towards the Earth during this month, making it appear much larger than the south pole. In the second half of August a large 'dark' area appeared on the solar disc, and was identified by the author (with a quick-look spectral analysis) as a large equatorial coronal hole, and named 'Elephant's Trunk' (or 'tusk'), because of its appearance. Figure 4.1 (central part) shows a CDS Mg IX image of the Elephant's Trunk on August 26th 1996.

A series of CDS observations of the Elephant's Trunk was carried out during the last week of August 1996, following the passage of the hole across the disc. These observations are outlined in Section 4.2.2.

4.2.1 The Whole Sun Month (WSM) campaign

Equatorial regions above the east/west limb

A series of four LIMB studies was used in order to cover a $4'$x$16'$ area. Figure 4.2 shows a mosaic image made in the Mg IX 368 Å line at the West limb on 1996 August 26. Observations like this were made regularly every few days from 12th August to 8th September 1996. Observations on the East limb were performed on August 13, 20, 27, 30, and September 3, 6. Observations on the West limb were made on August 12, 15, 19, 22, 26, 29, and September 2, 8.

Typically, these NIS observations were supported by GIS observations, a small slit scan across the limb in the E-W direction (G2AL study), and a long slit scan (GWEST and GEAST studies), to observe the corona at larger distances from the Sun, as shown in Figure 4.2.

Since the long slit GIS observations were un-calibrated, and in general to check the GIS calibration, various sets of observations were planned and executed by the author (although not analysed yet). These include slit $2''$x$2''$- $4''$x$4''$checks (using the TEST5_2 and MICRO studies) and $4''$x$4''$- $2''$x$240''$checks (using the GISAT_S and RWPM_1 studies).

A few observations with the large $90''$x$240''$ slit were also carried out in support. Movies have been created, that show the highly dynamic nature of all the solar structures observed,

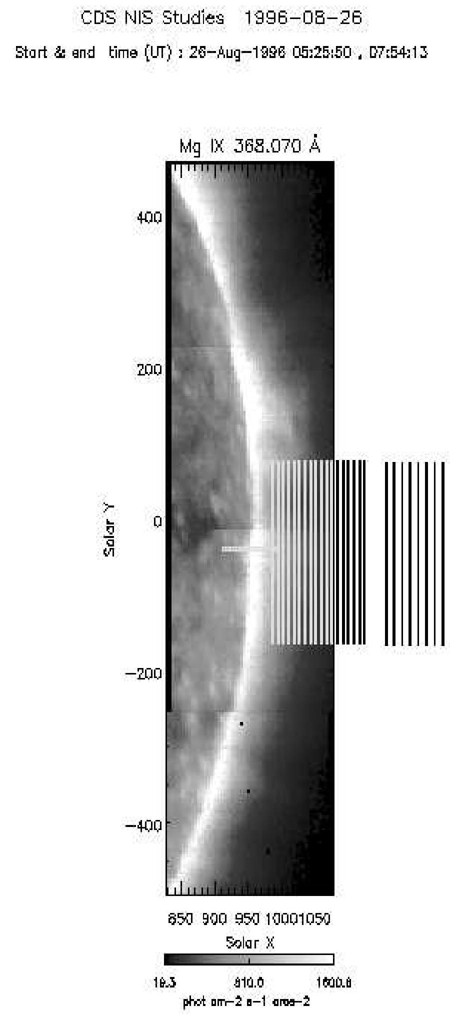

Figure 4.2: *A mosaic of four Mg IX 368 Å images taken by CDS at the Sun's west limb on August 26, 1996, showing also the position of the GIS studies, small and long slits.*

as seen off-limb.

Polar coronal holes

The observations over the polar coronal holes were a combination of observations planned by the author and those planned for the WSM.

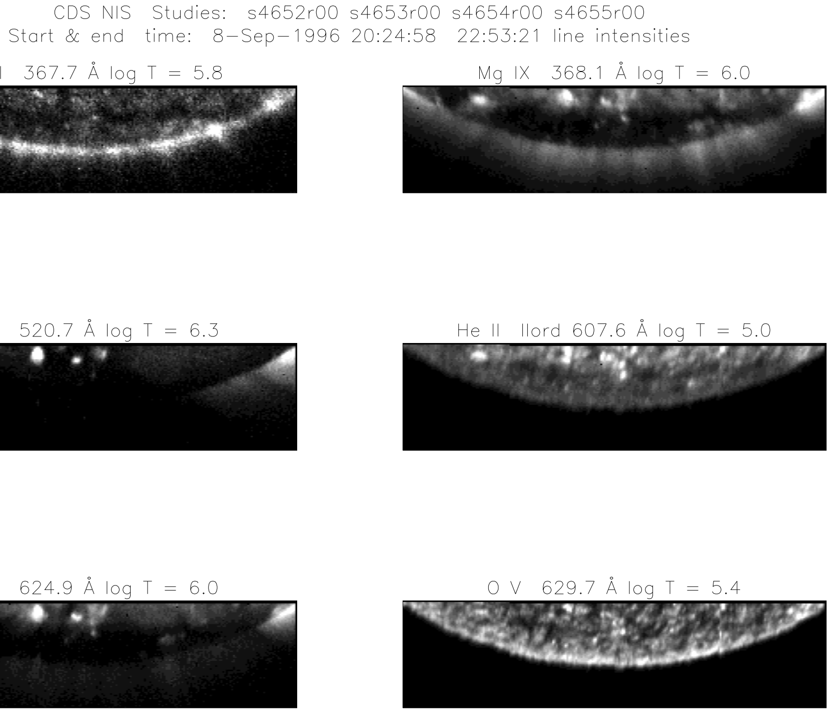

Figure 4.3: *A mosaic of four LIMB studies taken on September 8, 1996, in the south coronal hole. The total area in each panel is about* $16' \times 4'$.

In this case, a series of four LIMB studies was used to cover a $16' \times 4'$ area, as a mapping to study the structure and evolution of the coronal holes, and as 'context' observations for more detailed studies. Figure 4.3 shows mosaics created from the September 8 1996 observations. The upper transition region (Mg VII) and lower corona (Mg IX) lines show the presence of polar plumes. Observations of this type were made on August 10, 16, 17, 24, 25, 31, and September 7 to observe the north coronal hole. Observations of the south coronal hole were made on August 11, 18, and September 1, 8. In some cases, these observations were supported by GIS scans across the limb.

4.2.2 The Elephant's trunk

Figure 4.4 shows a magnetogram (SOHO/MDI) and an EUV image (SOHO/EIT) of the Sun taken on 26th August 1996. The Elephant's Trunk appeared as a predominantly

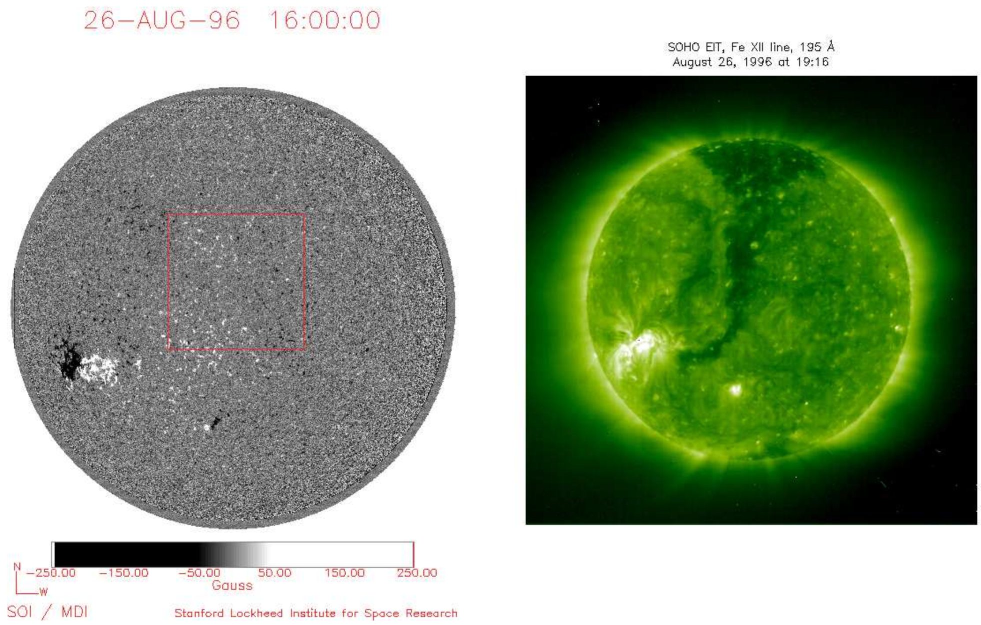

Figure 4.4: *The Elephant's Trunk as seen on the 26th August 1996. Left: a magnetogram from SOHO/MDI (courtesy of C. DeForest). Right: a SOHO/EIT image.*

unipolar region, that extended from the north coronal hole to a region of strong magnetic field associated with an active region just south of the equator. This field had the same polarity as the north polar hole. A neutral line appears to run along the prominence channel parallel to the coronal hole to the East. This equatorial coronal hole resembled the famous 'Italy boot-shaped' (CH 1) coronal hole observed by Skylab in 1973 and described in Chapter 1.

The Elephant's Trunk provided a rare and important opportunity to study coronal holes because:

- it crossed the Sun centre, making it possible to perform spectroscopic observations with a largely radial line of sight. Thus it was possible to observe the coronal hole, without contamination from foreground quiet sun material.
- The Sun was at solar minimum. Therefore, any contamination from foreground quiet sun material was further minimised.

A series of CDS observations of the Elephant's Trunk was carried out on the 25th, 26th, 27th, and 29th of August 1996.

A series of NIS observations (LIMB studies) were made on the 25th, 26th and 29th of August 1996 in order to create composite monochromatic images and to give an overall picture of the coronal hole. Figure 4.5 shows the CDS mosaics in Mg IX, created from

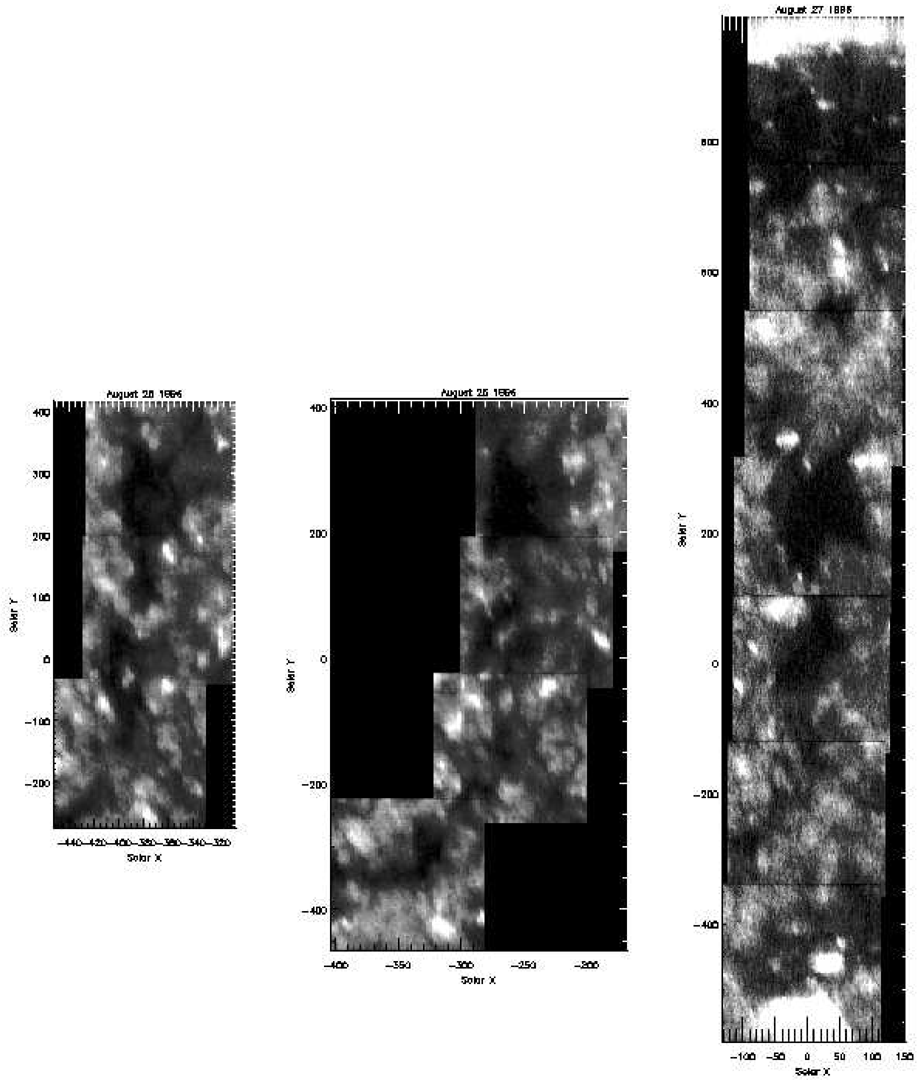

Figure 4.5: *The Elephant's Trunk as seen on the 25th 26th and 27th August 1996 in the coronal line Mg IX 368 Å by CDS, showing changes over the time-scale of one day.*

observations taken on the 25th, 26th and from a SYNOP sequence of 27th August. Small changes in the boundaries and inside the hole were visible on all time-scales, making it difficult to perform accurately pointed observations. The overall structure of the Elephant's Trunk, however, persisted for a long time. In fact, the hole largely decayed over a time scale of the order of two solar rotations, with parts remaining for much longer.

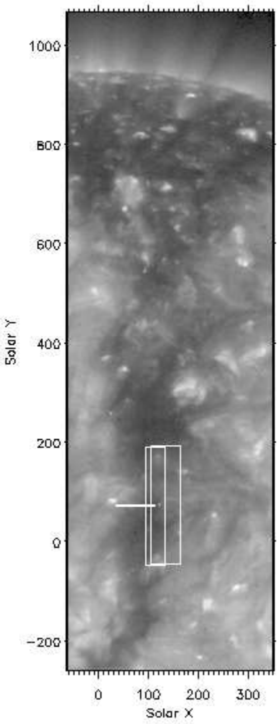

Figure 4.6: *EIT 195 Å – 27th August 1996 12:15 UT with the regions rastered by CDS. The CHBOPT2 is the rectangular region on the right, while the narrower NISAT_S5, partly overlapping, is on the left. A GIS E-W scan across the hole is also shown.*

A region near the solar equator was observed on the 25th, 26th and 27th, as it rotated across the meridian, using CHBOPT2 and NISAT_S5. Figure 4.6 shows the position of the rasters for the 27th. On the same days, some E-W GIS scans across the hole were obtained with the $4''$x$4''$slit, to observe both the east and west boundaries. Specific simultaneous observations with other instruments on board SOHO were also organised on the 27th, the day of the meridian passage. EIT and MDI observed the hole with high time and spatial resolution. SUMER produced reference spectra.

On the 29th, a GIS scan inside the hole, in the N-S direction was obtained, together with a NISAT_S5 raster.

4.3 The observations during September-October 1997

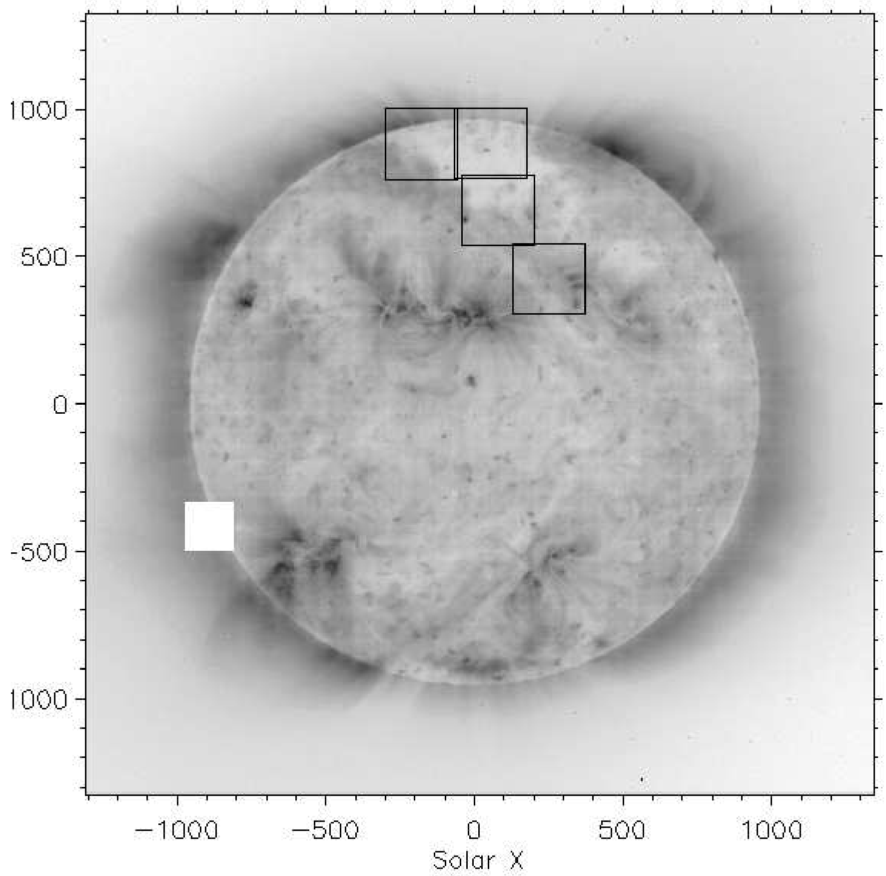

Figure 4.7: *EIT 195 Å – 7th October 1997, with the regions rastered by CDS. Negative image created with the IDL routine IMAGE_TOOL.*

During this period the Sun was in the rise phase of cycle 23. In the corona (see Figures 4.7, 4.8, and 4.9), many new active regions were forming at high-latitudes, and both polar holes were much reduced in area, with a bright polar crown region, emitting also high-temperature lines. The Sun was tilted in such a way that the north polar hole was more visible than the southern hole, which disappeared at times. A coronal hole Campaign (# 1990) was organised by B. Bromage and the author, with supporting ground observations and observations by the other SOHO instruments, in particular SUMER, EIT, and MDI. Mostly, the observations were of the north polar region, with meridian studies and with studies that followed the same region day by day. In particular, an extension of the polar hole, and a region in the N-W were studied in more detail. As in August 1996, mapping of the coronal holes was performed with large field-of-view NIS rasters (as shown in Figure 4.7), while more detailed observations were made using smaller field-of-view GIS and NIS observations. Figure 4.8 shows as an example the sequence of areas observed on the 2nd October 1997 with the WIDE3LA1, UCLAN_N3, DEM_GIS, NSGSCAN1 studies, to observe the boundary of the north coronal hole, at the meridian (special SUMER support was also organised).

There were some periods of high-telemetry, when special sequences were run. Many full-wavelength spectra were taken (NISAT_S5, UCLAN_N2 studies) over the boundary of the north coronal hole. In particular, on the 14th of October, UCLAN_N2 was repeated 6 times on the same area. Also, various high-rate GIS E-W scans (HRBNDWE study) were run over coronal hole regions, including plumes. On the 17th of October one of these scans was done above the north limb.

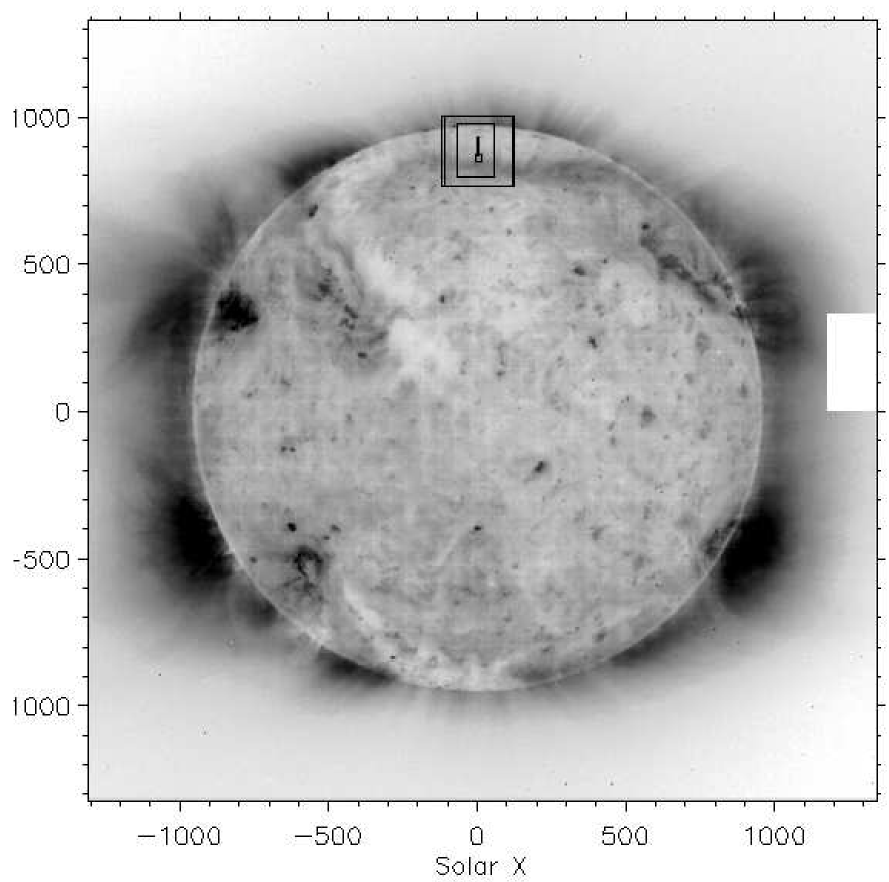

Figure 4.8: *EIT 195 Å – 2nd October 1997, with the regions rastered by CDS. Negative image created with the IDL routine IMAGE_TOOL.*

During the last week of September, some observations were performed in off-limb regions, in support of EISCAT IPS observations, together with LASCO observations.

In order to study the relationship between the observed features at radio and EUV wavelengths (see *Gopalswamy et al.*, 1998), specific CDS simultaneous observations with the Nobeyama Radio telescope were planned, in collaboration with Dr. Gopalswamy. Mainly, the NIS WIDE3LA1 study, which is composed of three scan positions with the wide slit, was used to build movies in the brightest He I, O V, Mg IX lines seen by CDS. Simultaneous observations on October 10–11th, 14–15th were executed and analysed.

4.4 Off-limb observations of polar holes (February - April and October 1997)

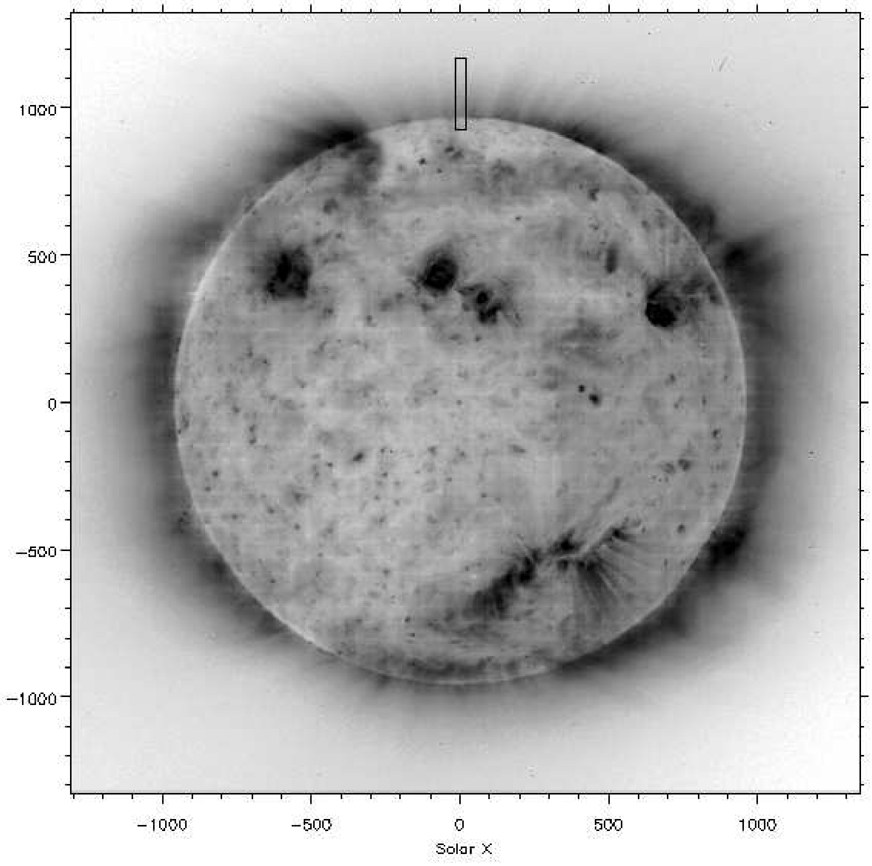

Figure 4.9: *EIT 195 Å – 12th October 1997 17:26 UT, with the off-limb NISAT_S5 raster positions. The NIS observations started at 8:55 UT and ended at 13:43 UT. Negative image created with the IDL routine IMAGE_TOOL.*

To take advantage of high-telemetry, on the 12th of October 1997, a series of 6 NISAT_S5 studies were taken off-limb in an inter-plume region (see Figure 4.9). This sequence of rasters represents the longest off-limb full-spectrum NIS observation taken by CDS, as far as the author is aware. The solar corona at that time was such that any effects of plasma from extended hot loops overlying the coronal holes were very limited, as can be seen in the EIT picture in Figure 4.9, and therefore most of the observed emission comes from the inter-plume region.

A few GIS N-S scans over the north or south polar limbs were performed. In addition, a particular set of observations was developed to study plume and inter-plume regions off-limb, and named *'off-limb cross'*. The main idea was to perform one N-S scan just

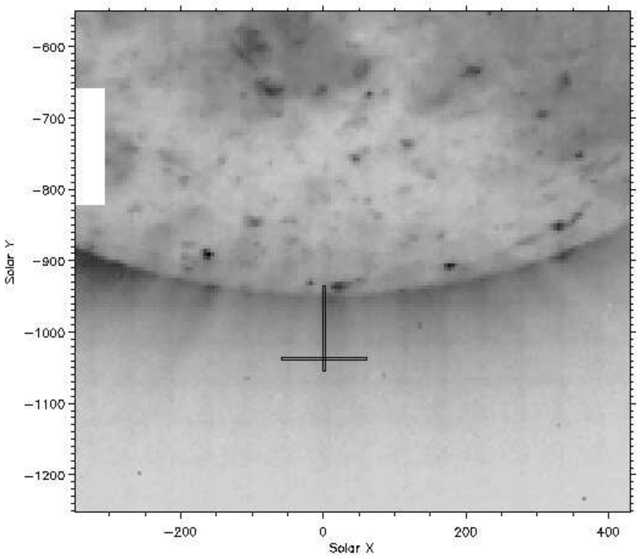

Figure 4.10: *EIT 195 Å – 27th March 1997 12:49 UT, with the GIS 'off-limb cross' rasters. Negative image created with the IDL routine IMAGE_TOOL.*

off-limb and one E-W scan at larger distances, to form a cross (see Figure 4.10) centred at the meridian. Since the error in the CDS pointing ($10''$) is of the order of the plume dimensions ($20''$), such a combination of two rasters was designed to check the pointing. The N-S raster was pointed to have a few exposures inside the limb, and therefore to be able to check its Solar Y position. From the E-W scan it is possible to distinguish between plume and inter-plume areas, since the plumes (if there are any) are aligned along the N-S direction around the meridian. The Solar Y (i.e. the distance from the limb) of this raster could easily be checked with the help of the N-S raster, because the intensities of the lines have an exponential fall-off with distance making it easy to find the intersection of the two rasters.

The exposure times, distances and length ($120''$) of the rasters were adjusted to be able to observe on average at least one plume and inter-plume region as far as possible from the limb, with good signal-to-noise and with a total duration (about 7h) not too long, so that effects of the solar rotation (which are minimal on the meridian at the poles) would be negligible.

Observations such as that shown in Figure 4.10 were repeated on the 13th February, 10th March (this had missing data and wrong pointing), 29th March (again with large data dropouts), 1st April 1997, and the 23rd October, all in 1997.

4.5 The software developed for the data analysis

This Section gives a short description of the procedures developed for the analysis of the CDS data and of the software that was written in IDL by the author. Basic software was available to read the data, perform the standard corrections (such as flat-fielding), and the line fitting (which became available only in 1997), as described in Chapter 3. The high versatility of the CDS instrument, in terms of type of observations, meant that each CDS study (or sequence of studies) required the development of appropriate analysis software. A set of programs was written with the flexibility to automate and simplify the data analysis of as many CDS studies as possible. IDL routines were also written for other purposes, some of which (e.g. CDS calibration or DEM analysis) have already been described. About 200 IDL routines containing a total of more than 100 000 lines of code were written. Some of the software has been released for public use (the DEM package, *Del Zanna et al.*, 1997), and some has been distributed as part of international collaborations. Only a short description of some of the software used in this thesis is given here, to give an idea of the type of problems encountered and how they have been solved.

The data analysis of a single observation.

Each single CDS observation is stored as a FITS file. Routines were written to perform the *first step standard analysis* on the raw data, applying one-by-one all the corrections that have been described in Chapter 3, with various options, plots and checks. Depending on which instrument was used, on the type of raster (e.g. one-dimensional or bi-dimensional for the GIS), and on the type of data extraction, an appropriate routine had to be written. In the NIS case, contiguous windows (if any) are merged. Then, the background is estimated and line intensities found, by summing the pixel values and/or applying the multiple line fitting described in Chapter 3. The results are then saved in IDL 'save files'. Routines were written to display the results in various ways, and to perform subsequent analyses on the data.

The data analysis of a series of FITS files

In many cases a 'single' observation consisted of a series of FITS files, that had to be processed one by one, and then combined. The complexity of the data processing followed the complexity of the type of CDS study. Among the most complex and time consuming for the data analysis, were the CHBOPT2 and the HRBNDWE studies.

The mosaics of the data

Mosaics of the monochromatic images were formed from the single observations, interactively adjusting the relative position of each one to obtain the best composite image.

Specific features (such as the solar limb in chromospheric lines) that do not change in time, were usually used for this purpose. The IDL save files of the single observations were read and then the combined data were saved in a new IDL save file. Other routines were written to perform subsequent analyses on the merged data. These include displays of the images and ratios of any two of them, examination of the results, selection of areas to average, production of line fitting, and storage of the results in various forms.

The selection of areas to average

In most cases, even long exposures were not enough to achieve sufficient signal, in particular in coronal holes, and averaging of spectra was needed to improve the signal-to-noise in the weak lines, especially the density-diagnostic ones. For the off-limb observations, software was developed to interactively select areas to spatially average spectra along concentric arcs at fixed heights above the limb, to provide a one-dimensional, radial dependence of the spectra (after the gaussian fitting of the line intensities). It is also possible to select a range of position angles, in order to select regions of different latitudes. The software also allows selection of an intersection of these concentric areas and other areas selected by other criteria (e.g. to include only an inter-plume region or to exclude an active region). For the on-disc case, software was written to select areas, add them, 'intersect' and overplot them, in order to produce a single spectrum, or a sequence of spectra along one spatial direction.

In summary, specific customised analysis software needed to be written to deal with the various analyses, depending on which type of region was selected (e.g. a single region or a sequence of regions), which instrument was used (i.e. NIS or GIS), and which type of observation was made (e.g. full- or windowed-spectrum for NIS).